CellPress

Cell Metabolism
Article

Mutation of Nogo-B Receptor, a Subunit of *cis*-Prenyltransferase, Causes a Congenital Disorder of Glycosylation

Eon Joo Park,[1,6] Kariona A. Grabińska,[1,6] Ziqiang Guan,[2] Viktor Stránecký,[3] Hana Hartmannová,[3] Kateřina Hodaňová,[3] Veronika Barešová,[3] Jana Sovová,[3] Levente Jozsef,[1] Nina Ondrušková,[4] Hana Hansíková,[4] Tomáš Honzík,[4] Jiří Zeman,[4] Helena Hůlková,[3] Rong Wen,[5] Stanislav Kmoch,[3,*] and William C. Sessa[1,*]

[1]Department of Pharmacology and Vascular Biology and Therapeutics Program, Yale University School of Medicine, 10 Amistad Street, New Haven, CT 06520, USA

[2]Department of Biochemistry, Duke University Medical Center, DUMC 2927, Durham, NC 27710, USA

[3]Institute for Inherited Metabolic Disorders, First Faculty of Medicine, Charles University and General University Hospital, Ke Karlovu 2, Prague 2, 128 08 Czech Republic

[4]Department of Pediatrics, First Faculty of Medicine, Charles University and General University Hospital, Ke Karlovu 2, Prague 2, 128 08 Czech Republic

[5]Bascom Palmer Eye Institute, University of Miami, Miller School of Medicine, 900 NW 17th Street, Miami, FL 33136, USA

[6]Co-first author

*Correspondence: skmoch@lf1.cuni.cz (S.K.), william.sessa@yale.edu (W.C.S.)

http://dx.doi.org/10.1016/j.cmet.2014.06.016

SUMMARY

Dolichol is an obligate carrier of glycans for N-linked protein glycosylation, O-mannosylation, and GPI anchor biosynthesis. *cis*-prenyltransferase (*cis*-PTase) is the first enzyme committed to the synthesis of dolichol. However, the proteins responsible for mammalian *cis*-PTase activity have not been delineated. Here we show that Nogo-B receptor (NgBR) is a subunit required for dolichol synthesis in yeast, mice, and man. Moreover, we describe a family with a congenital disorder of glycosylation caused by a loss of function mutation in the conserved C terminus of NgBR-R290H and show that fibroblasts isolated from patients exhibit reduced dolichol profiles and enhanced accumulation of free cholesterol identically to fibroblasts from mice lacking NgBR. Mutation of NgBR-R290H in man and orthologs in yeast proves the importance of this evolutionarily conserved residue for mammalian *cis*-PTase activity and function. Thus, these data provide a genetic basis for the essential role of NgBR in dolichol synthesis and protein glycosylation.

INTRODUCTION

Nogo-B receptor (NgBR) was identified via expression cloning as a protein that interacts with the N terminus of Nogo-B, also called reticulon-4b (Miao et al., 2006). NgBR is a polytypic membrane protein, and its C-terminal domain shares significant homology with two gene products: (1) NUS1, a gene in yeast required for survival and N-glycosylation (Harrison et al., 2011; Yu et al., 2006) and (2) *cis*-prenyltransferases (*cis*-PTase), including genes in yeast (*RER22* and *SRT1*), a human ortholog, (*hCIT*, also called dehydrodolichol diphosphate synthase [*DHDDS*]), and bacterial undecaprenyl pyrophosphate synthase (*uppS*) (Sato et al., 1999; Schenk et al., 2001; Surmacz and Swiezewska, 2011). In lower organisms, single subunit *cis*-PTases such as UPPS catalyze the condensation reactions of isopentenyl pyrophosphate (IPP) with farnesyl pyrophosphate (FPP) to synthesize linear polyprenyl pyrophosphate with specific chain lengths. Polyprenyl pyrophosphate is dephosphorylated into polyprenol and then reduced by a polyprenol reductase to produce dolichol (Cantagrel et al., 2010). In mammals, the relative contribution of Nus1/NgBR versus Rer2/Srt1/hCIT to *cis*-PTase activity and dolichol synthesis is unknown since loss of function of each grouping of genes results in reduced glycosylation.

Congenital disorders of glycosylation (CDG) are genetic diseases that represent an extremely broad spectrum of clinical presentations due to defects in several steps of protein glycosylation. Recently, there have been several reports of genetic defects in the dolichol biosynthetic pathway, such as mutations in *DHDDS*/*hCIT* and *SRD5A3* (Cantagrel et al., 2010; Kasapkara et al., 2012; Zelinger et al., 2011; Züchner et al., 2011). DHDDS-CDG is associated with inherited retinitis pigmentosa, a disorder causing retinal degeneration, and DHDDS-CDG patients did not show the other typical CDG symptoms. SRD5A3-CDG affects the final step in dolichol synthesis. Its clinical features are typical for CDG type 1 glycosylation disorders, including psychomotor retardation, ocular malformations, cerebellar hypoplasia, skin lesions, and facial dysmorphism.

Here, we characterize the dolichol biosynthesis pathway in mice and yeast and demonstrate the necessity of both hCIT and NgBR for dolichol biosynthesis. In addition, we describe a unique congenital disorder of glycosylation caused by a mutation in NgBR, a conserved subunit of *cis*-PTase. Patients harboring a R290H mutation of NgBR have congenital scoliosis, profound psychomotor retardation, refractory epilepsy, and macular lesions showing retinitis pigmentosa. Thus, hCIT/NgBR heteromers are essential, conserved components of the machinery necessary for glycosylation reactions in mammals.

RESULTS AND DISCUSSION

Targeted Disruption of *NgBR* Causes Early Embryonic Lethality In Vivo and Defective *cis*-PTase Activity and Cholesterol Levels in Isolated Fibroblasts

To examine the physiological significance of NgBR, we generated a conditional knockout mouse (Figures S1A–S1C available online). The *NgBR* knockout allele ($NgBR^{\Delta}$) was generated by crossing *NgBR* conditional allele ($NgBR^{f}$) with a protamine Cre driver expressed in the male germline (O'Gorman et al., 1997). Heterozygous NgBR mice ($NgBR^{\Delta/+}$) appeared normal, and intercrosses with $NgBR^{\Delta/+}$ showed no viable homozygous mice ($NgBR^{\Delta/\Delta}$) (Figure 1A). To determine when lethality occurred, timed pregnancies of $NgBR^{\Delta/+}$ breeding were examined at embryonic day 6.5 (E6.5) and E7.5. No $NgBR^{\Delta/\Delta}$ embryos were identified at these time points indicating postimplantation embryonic lethality before E6.5 (Figures 1B and 1C). Next, we established mouse embryonic fibroblasts (MEFs) cultured from $NgBR^{f/f}$ mice using an inducible Cre-loxP system. Reduced expression of NgBR in the tamoxifen inducible NgBR knockout (NgBR iKO) MEF cells was confirmed by PCR and western blotting for mRNA and protein levels, respectively (Figure S1D). NgBR iKO MEFs showed accumulation of free cholesterol as determined by filipin staining (Figure 1D), decreased *cis*-PTase activity in isolated membranes (Figure 1E), and mannose incorporation into protein (Figure 1F). Transduction of cells with lentiviral human NgBR rescues the increase in free cholesterol (Harrison et al., 2009) and the decrease in mannose incorporation (Figures 1E and 1F). Furthermore, we exposed cells to lovastatin, an inhibitor of 3-hydroxy-3-methylglutaryl-coenzyme A (HMG-CoA) reductase, the rate-limiting enzyme in the synthesis of isoprenoids, and measured cell viability using an MTT assay. NgBR iKO MEF cells were significantly more sensitive to lovastatin than control MEF cells (Figure 1G). Since defects in protein glycosylation can induce the unfolded protein response (UPR), activation of the UPR pathway in wild-type (WT) and NgBR iKO MEF cells was examined by RT-PCR for marker genes of the pathway, including *Bip*, *Chop*, and *Chac* (Figure 1H). All three genes were markedly increased in NgBR iKO MEFs, implying that defects in dolichol synthesis and protein glycosylation were activating the UPR pathway of ER stress. Thus, NgBR is essential for early development and *cis*-PTase activity in vivo.

Heteromeric Organization of *cis*-Prenyltransferase Is Conserved between Fungi and Mammals

The eukaryotic *cis*-PTase was initially presumed to be a homodimer based on studies of UPPS of *E. coli* and *M. luteus* (Fujihashi et al., 2001; Guo et al., 2005). Our previous work demonstrated that hCIT or NgBR were necessary for *cis*-PTase activity (Harrison et al., 2011). However, we did not provide unequivocal evidence that NgBR is indispensable for enzymatic complex formation and activity. To definitively dissect the roles of NgBR and hCIT as components of *cis*-PTase activity, we characterized the yeast orthologs (in *S. cerevisiae* and *S. pombe*) of NgBR and hCIT using genetic and biochemical approaches. We hypothesized that baker's yeast may have two heteromeric *cis*-PTase complexes: Nus1-Rer2 and Nus1-Srt1. To test this, we generated a triple deletion strain, *nus1Δ, rer2Δ, srt1Δ*, expressing the homomeric *cis*-PTase from *Giardia lamblia* (Glc*is*PT) to support growth (Grabińska et al., 2010). Indeed, we were able to isolate yeast cells lacking chromosomal copies of *NUS1*, *RER2*, and *SRT1* genes but bearing instead Glc*isPT* on a plasmid with a *URA3* marker (Figure 2A). To examine conservation of the heteromeric structure of *cis*-PTases, the triple deletion strain was transformed with *MET15* and *LEU2* plasmids bearing the cDNAs indicated in Figure 2A. As expected, viable strains were obtained after expressing *NUS1/RER2* or *NUS1/SRT1* as positive controls (Figure 2A). In addition, *NUS1* is also compatible with Sp*rer2* or *hCIT*, *Spnus1* with Sp*rer2*, Sp*nus1*with *hCIT*, and *NgBR* with *hCIT* only. Reverse-phase thin-layer chromatography (TLC) of polyprenols generated from membranes isolated from wild-type BY4742 or transformed mutant cells revealed that human and *S. pombe* enzymes synthesize polyprenols similarly to that in their parental organisms (Figure 2B). However, the size of the dominant polyprenol pyrophosphate synthesized by the hybrid enzymes varied, implying that the different gene products (*NgBR/Nus1* and *hCIT/Rer2/Srt1*) determined polyprenol chain length.

To examine the enzymatic activities of the gene products, we used in vitro translation (IVT) followed by *cis*-PTase assays on the above combinations of the *cis*-PTase components. Enzymes present in the IVT mixture were able to incorporate ^{14}C-IPP into short prenols up to 6 units (Figure 2C, first column) but were unable to synthesize longer chain polyprenyl pyrophosphates. Expression of Nus1, Rer2, or mixtures of IVT Nus1 with Rer2 products in equal amounts (as shown by western blotting in the bottom panel) did not catalyze formation of polyprenols. Interestingly, only cotranslation of Nus1 with Rer2 and its orthologs in *S. pombe* or humans formed an active *cis*-PTase complex producing prenols of expected lengths (Figures 2C–2F, lane 5), indicating that both proteins are required for a functional enzyme (Figures 2D–2F). Collectively, the data support the heteromeric structure of mammalian and yeast *cis*-PTase and suggest that eukaryotic *cis*-PTase is assembled during translation since only cotranslation, but not mixing of the proteins, yields active enzyme. Taken together, these data provide a clear rationale for the role of *RER2/NUS1* and related genes in dolichol biosynthesis and advance our understanding of this important pathway.

A Mutation on NgBR Causes Congenital Scoliosis, Severe Neurological Impairment, Refractory Epilepsy, Hearing Deficit, and Visual Impairment

Recently, exome sequencing of individual families with symptoms of a congenital disorder of glycosylation (CDG) has led to the discovery of mutations in DHDDS (hCIT) and SRD5A3, genes involved in the early steps of polyprenol synthesis (Cantagrel et al., 2010; Kasapkara et al., 2012; Zelinger et al., 2011; Züchner et al., 2011). DHDDS-CDG is associated with inherited retinitis pigmentosa, a disorder causing retinal degeneration, and SRD5A3-CDG patients exhibit psychomotor retardation, ocular malformations, cerebellar hypoplasia, skin lesions, and facial dysmorphism. In our clinic, a family of Roma origin (Figure 3A) composed of healthy, unrelated parents and four siblings was examined, and two siblings presented with congenital scoliosis, severe neurological impairment, refractory epilepsy, hearing deficit, and visual impairment with discrete bilateral macular lesions.

A

Stage	*NgBR* $^{+/+}$	*NgBR* $^{+/\Delta}$	*NgBR* $^{\Delta/\Delta}$
E6.5	10	13	0
E7.5	27	41	0
3 weeks	22	55	0

B

E7.5	with embryo	in resorption
No. of decidua	58	19
Actual %	75.3	24.7
Expected %	75	25

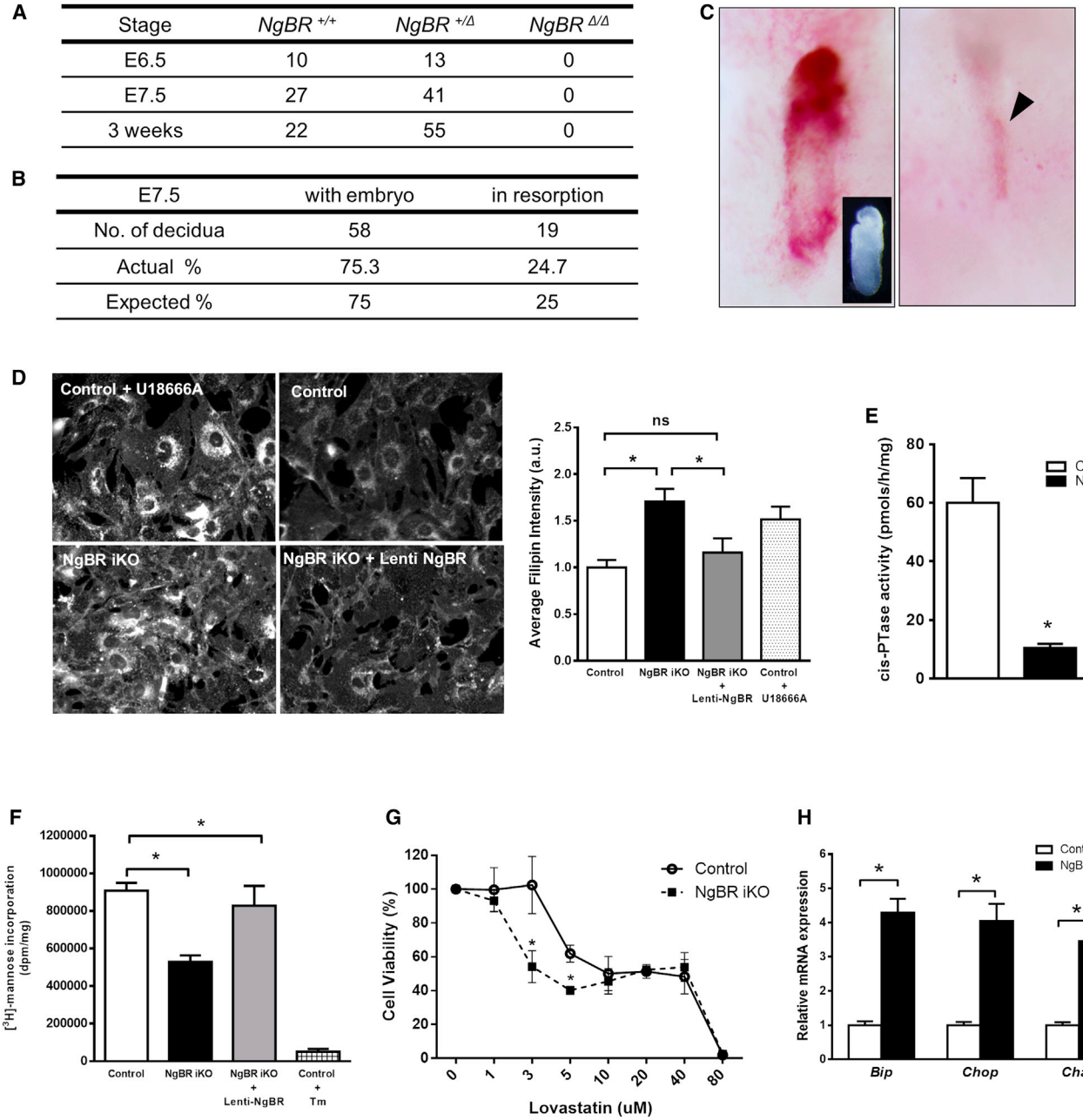

Figure 1. Characterization of NgBR Knockout Mouse Embryos and Fibroblasts

(A) Genotype obtained from the progeny of heterozygous mating. No NgBR$^{\Delta/\Delta}$ embryo was detected.

(B) Embryo resorption frequencies during postimplantation development. Resorption sites were apparent at E7.5 among ~25% decidua.

(C) Representative decidua of E7.5 embryo resorption sites analyzed. Decidua were obtained from NgBR$^{\Delta/+}$ × NgBR$^{\Delta/+}$ breeding. Decidua with embryo contained normally developed E7.5 embryo (insert). Presumptive NgBR$^{\Delta/\Delta}$ decidua exhibit implanted site for embryo without evident embryonic material (arrowhead).

(D) Filipin staining and quantitative representation for MEF. Filipin staining was performed 48 hr after Lenti-NgBR transduction into NgBR iKO MEF cells. U18666A was used as a positive control for inhibition of cholesterol trafficking.

(E) Microsomal *cis*-PTase activity assay for NgBR iKO MEF. Enzyme activity was reduced by 83% in NgBR iKO MEF compare to control.

(F) [2-^{3}H]-mannose labeling of proteins in mouse embryonic fibroblasts. Tunicamycin (Tm) treatment was used as a control.

(G) Statin sensitivity measured by MTT assay. Cell viability was determined by MTT assay after 16 hr exposure with various concentrations of lovastatin (1–80 μM). Cell viability was calculated by the following equation: MTT optical density value of treated sample / MTT OD value of nontreated sample.

(H) RT-PCR for UPR pathway genes. Relative mRNA expression to control show increased expression.

Data are representative of at least three experiments. *$p < 0.05$. Data are mean ± SE. See also Figure S1.

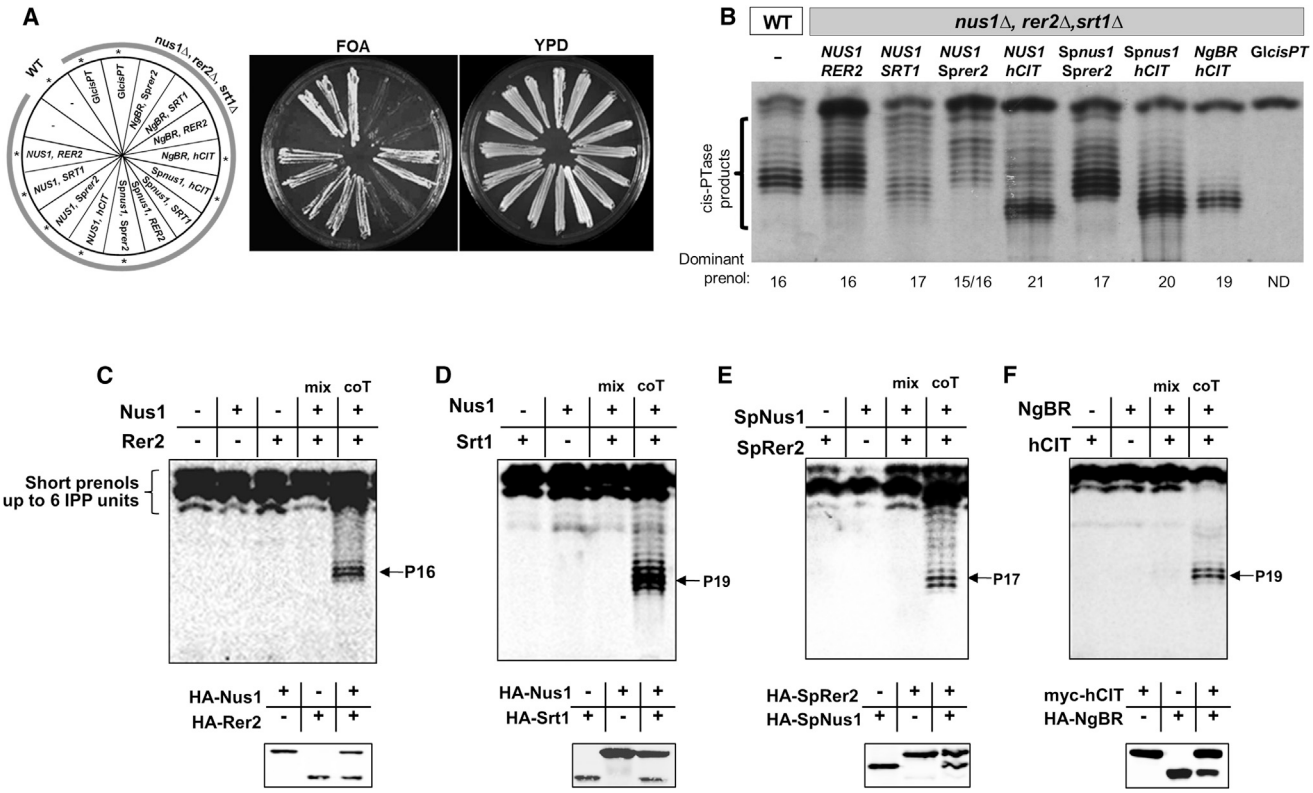

Figure 2. Mammalian and Fungi *cis*-PTase Is a Heteromer Consisting of NgBR/Nus1 and hCIT/Rer2/Srt1 Orthologs

(A) *The rer2Δ, srt1Δ, nus1Δ* triple deletion strain expressing *G. lamblia cis*-PTase from *URA3* plasmid was transformed with the respective plasmids as indicated. The cells were streaked onto complete plates (YPD) or synthetic complete medium containing 1% 5-fluoroorotic acid (FOA). The Ura3 protein, which is expressed from the URA3 marker present in the plasmids, converts FOA to toxic 5-fluorouracil. The viable combination of genes was marked with asterisks.

(B) In vitro *cis*-PTase assay. Reverse-phase TLC of polyprenols from membranes prepared from wild-type BY4742 (WT) or triple mutant expressing the respective plasmids for hybrid *cis*-PTases supporting growth of the triple knockout strain.

(C–F) Reverse-phase TLC of polyprenols from *cis*-PTase activity assay by Nus1/Rer2 (C), Nus1/Srt1 (D), SpNus1/SpRer2 (E), or NgBR/hCIT (F) expressed in IVT. Assays were done according to standard conditions using 20 μl of IVT for *cis*-PTase activity. Reaction products were extracted and developed on high-performance TLC (HPTLC) RF18 plate. Expression of the HA- or myc-tagged proteins was verified by western blotting of the reaction mix. coT, cotranslation. Data are representative of at least three experiments.

Proband II.3 was born at term with intrauterine growth retardation. Muscle hypotonia was present since birth, and congenital scoliosis and developmental delay were observed since early infancy. Tonic-clonic seizures, refractory epilepsy, and recurrent attacks of status epilepticus developed from the age of 11 months. Microcephaly (3rd centile), failure to thrive (<3rd centile), regression of psychomotor development, severe axial hypotoniab and acral spasticity developed after discharge. Routine laboratory tests were unremarkable, and cholesterol level was within reference range. The boy died at the age of 29 months. Histopathological findings in autopsy tissue revealed nonspecific neuronal loss in brain cortex and cerebellum. Similarly to his brother, proband II.4 had generalized hypotonia, congenital scoliosis, and significant delay in motor milestones. Refractory epilepsy started at the age of 7 months, and he has been hospitalized several times with severe seizures. He lost any social interaction, and he displays no spontaneous movements. At the age of 4 years, he has microcephaly (0.6th centile), failure to thrive (<5th centile), and marked hypertrichosis. He has severe axial hypotonia, acral spasticity with preserved deep tendon reflexes, pseudobulbar palsy, and central visual and hearing impairment. MRI of the brain revealed severe cortical atrophy. A complete dilated fundus examination including color fundus photography was performed under general anesthesia. At the age of 31 months, except for an opacity located in the inferior half of the right cornea, there were bilaterally no other anterior segment abnormalities, and the vitreous was optically clear. There were no bone spicule pigmentations, but diffuse retinal pigment epithelium mottling could be observed bilaterally. Optic nerves appeared paler and retinal vessels narrower. Repeated examination at the age of 4 years documented a development of bilateral macular lesion showing foveal hyperautoflorescence (Figure 3B).

The exomes of parents and both affected probands were sequenced and searched for genetic variants in the internal exome database, the Exome Variant Server, and 1000 Genomes databases, and only four such variants were discovered; three are located in the autozygous region identified on chromosome 6 and one on chromosome 21 (Table S1). Corresponding genes were evaluated based on their potential contribution to the clinical phenotypes, and a homozygous missense mutation c.869G > A in the *NUS1* (NM_138459) or NgBR was found. The

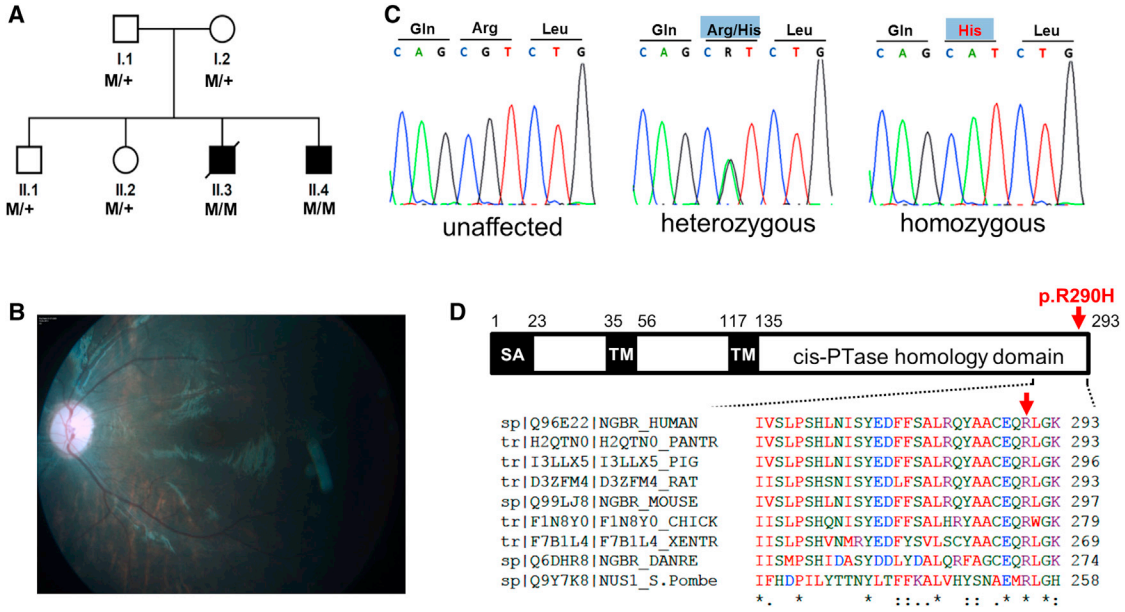

Figure 3. Identification of a Conserved Mutation in the NgBR Gene in Patients with a Constellation of Symptoms Consistent with a Glycosylation Disorder

(A) Pedigree of the Czech family. Black symbols denote affected individuals, open symbols denote unaffected parents and siblings. M/+ denotes presence (M) or absence (+) of the mutation as defined by Sanger sequencing.

(B) Dilated fundus photograph in proband II.4 reveals a granular yellow-white lesion in the fovea, pale optic nerve, and retinal vessels with signs of attenuation.

(C) Chromatograms of *NgBR* genomic DNA sequences showing identified mutations in the family. Left: sequence of the unaffected individual. Middle: sequence showing heterozygous mutation c.G869 > A in the heterozygous carrier. Right: sequence showing homozygous mutation c.G869 > A in one of the probands.

(D) Schematic representation of NgBR showing the protein primary structure, location of the p.R290H mutation, and amino acid sequence alignment of the C-terminal part of the protein. SA, putative signal anchor; TM, putative transmembrane domain. The amino acid residues are color coded: small amino acids are red, acidic in blue, basic in magenta, and hydroxyl with amine in green. See also Table S1.

c.869G > A mutation was confirmed by Sanger sequencing, and the affected probands are homozygous for this mutation, whereas their parents and healthy siblings are heterozygous (Figure 3C). The mutation encodes for amino acid exchange p.Arg290His (R290H), which is located in the evolutionarily conserved C-terminal domain of NgBR (Figure 3D) and is predicted to affect protein function with a score of 0.00 according to SIFT and to be damaging using Polyphen. This mutation was not reported in dbSNP, 1000 Genomes, or the Exome variant server and was not listed in our internal exome database (>250 exomes). Targeted genotyping of genomic DNA from 255 individuals of Roma origin identified two additional heterozygous carriers of the c.869G > A mutation. Even though the identity and relation status of these two carriers is unknown, this finding suggests that the congenital disorder of glycosylation caused by a loss-of-function mutation of NgBR may be relatively frequent among the European Roma population.

NgBR R290H Mutation Triggers Defects in Cellular Cholesterol Trafficking and Dolichol Biosynthesis

To characterize the NgBR R290H mutation, fibroblasts were isolated from control and NgBR R290H patients and we examined the levels of NgBR mRNA, protein, and interaction of NgBR with hCIT (Figures S3A–S3C). We did not observe any significant differences in the migration of NgBR on SDS-PAGE or the levels of NgBR protein compared to WT (Figure S1B). This suggests that the translation and the subsequent processing of mutant NgBR protein were not altered by the presence of the mutation. NgBR was isolated as a protein that interacted with reticulon 4B, also called Nogo-B (Miao et al., 2006). Therefore, we examined whether Nogo-B levels and its interaction with NgBR were altered in carriers of the NgBR mutation. The levels of Nogo-B, its interaction with NgBR, and the localization of Nogo-B were not different (Figures S3D–S3F). Next, we assessed three aspects of NgBR function, free cholesterol levels, *cis*-PTase activity, and glycosylation. WT cells had little filipin-positive free cholesterol, whereas treatment with U18666A to induce a Niemann-Pick C (NPC) disease phenotype (Cenedella, 2009) increased free cholesterol (Figure 4A, quantified in the right panel). In contrast, NgBR R290H mutant cells exhibited increased accumulation of free cholesterol similar to cells where NgBR was silenced (Harrison et al., 2009). Additionally, *cis*-PTase activity (Figure 4B) and mannose incorporation into proteins (Figure 4C) was markedly lower in NgBR R290H fibroblasts compared to control. We also examined defective glycosylation of proteins in patient fibroblasts by western blotting for two known glycoproteins, LAMP-1 and ICAM-1 (He et al., 2012; Xiang et al., 2013). Both LAMP-1 and ICAM-1 were hypoglycosylated in the patient fibroblasts (Figure 4D). Thus, the NgBR R290H mutant is a loss-of-function mutation that affects *cis*-PTase function of NgBR without disrupting complex formation with hCIT or Nogo-B. The reduced *cis*-PTase activity in fibroblasts was manifested as altered dolichol profiles in the urine or serum as assessed by mass spectrometry of all carriers of

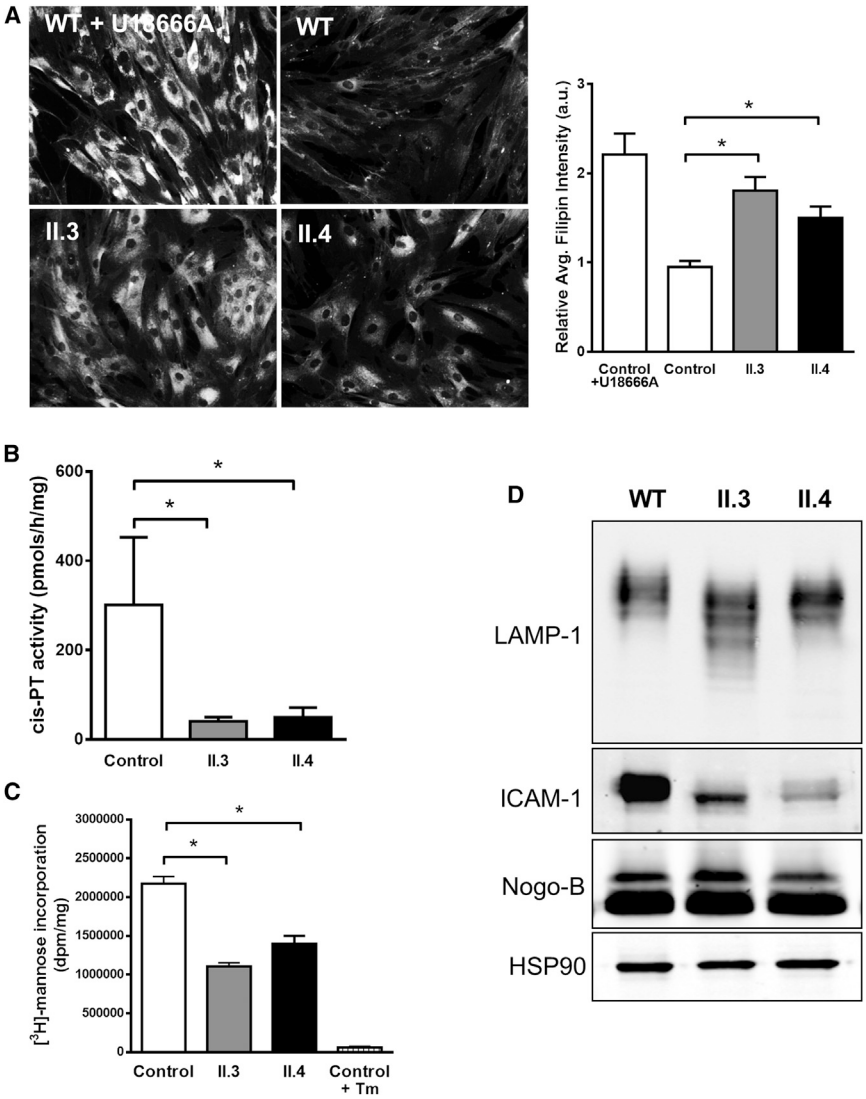

Figure 4. NgBR R290H Mutation Causes Defects in Cellular Cholesterol Trafficking and the Dolichol Biosynthesis Pathway

(A) Filipin staining and quantitative representation for human dermal fibroblast cells from patients (II.3 and II.4). U18666A was used as a positive control for inhibition of cholesterol trafficking.

(B) Microsomal *cis*-PTase activity using isolated membrane from fibroblasts. Compared to wild-type, less than 20% of activity was detected in the patient cells.

(C) [2-^{3}H]-mannose labeling of proteins. Cells were incubated with [2-^{3}H]-mannose for 4 hr, and TCA precipitated proteins were counted by scintillation. Tunicamycin (Tm) treatment was used as a control for loss of [2-^{3}H]-mannose incorporation into newly synthesized proteins. *$p < 0.05$. Data are mean ± SE, with $n = 4$ from three independent experiments.

(D) Western blot analysis of LAMP-1 and ICAM-1 levels in patient fibroblasts. Total lysates were analyzed, and the loading controls Nogo-B and Hsp90 are shown. See also Figure S2.

the R290H mutation (Figure S4), as recently described for patients harboring loss-of-function mutations in DHDDS(Wen et al., 2013).

Amino Acid at the Fourth Position from the C Terminus of NgBR Is a Functionally and Evolutionarily Conserved Residue

Alignment of NgBR orthologs from distantly related eukaryotic organisms reveals a high degree of conservation at the C terminus, with arginine or asparagine present at the fourth position from the C terminus (Figure 5A). To test the evolutionary conservation of this position, hCIT was expressed with NgBR or NgBR R290H in the *nus1Δ, rer2Δ, srt1Δ* triple knockout strain. Cells expressing the NgBR R290H allele have lower *cis*-PTase activity (Figure 5B), overall polyprenols (Figure 5C), and dolichol levels as measured by MS (Figure 5D). In addition, we analyzed *S. cerevisiae* and *S. pombe* Nus1 mutants to determine the importance of the amino acid conservation at the fourth position from the C terminus in NgBR orthologs. *S. cerevisiae* Nus1 belongs to group of fungi and plants NgBR orthologs bearing asparagine instead of arginine, while *S. pombe* Nus1 encodes arginine at position 255 corresponding to the R290 in human NgBR. Therefore, we compared *cis*-PTase activity of the *S. cerevisiae nus1Δ* strain expressing wild-type Nus1, Nus1-N372H (mimicking NgBR R290H mutation), as well as Nus1-N372R. Also, we expressed wild-type SpNus1 or SpNus1-R255H in the *nus1Δ* fission yeast strain. Mutation of the same position in Nus1 in *S. cerevisiae* (Figures 5E and 5F) and *S. pombe* (Figures 5G and 5H) resulted in a similar loss of function. Interestingly, the N372R allele of Nus1 from *S. cerevisiae* affects only the chain length of the product (Figures 5F) but not the rate of incorporation of IPP (Figures 5E).

Recently, altered ratios of plasma and urinary dolichols were observed in retinitis pigmentosa patients carrying the K42E mutation in DHDDS/hCIT (Wen et al., 2013). To compare the influence of NgBR R290H and hCIT K42E mutations on *cis*-PTase activity, we expressed hCIT or hCIT K42E with NgBR or NgBR R290H in the *S. cerevisiae* triple knockout strain and measured enzyme activity. Introduction of this mutant into the triple knockout strain expressing WT NgBR reduced steady-state *cis*-PTase activity to an extent similar to that of NgBR R290H expressed with WT hCIT (Figure 5I), and combining the mutations reduced activity, further demonstrating epistasis of the gene products.

NgBR and its orthologs are essential genes, and NgBR/hCIT heteromers are responsible for dolichol synthesis in mammalian cells (Figures 6A and 6B). Based on previous work, NgBR can interact with hCIT, NPC2, and Nogo-B (Figure 6B; numbered 1–3). The interaction with NPC2 was identified by an independent broad-based screening strategy (Harrison et al., 2009).

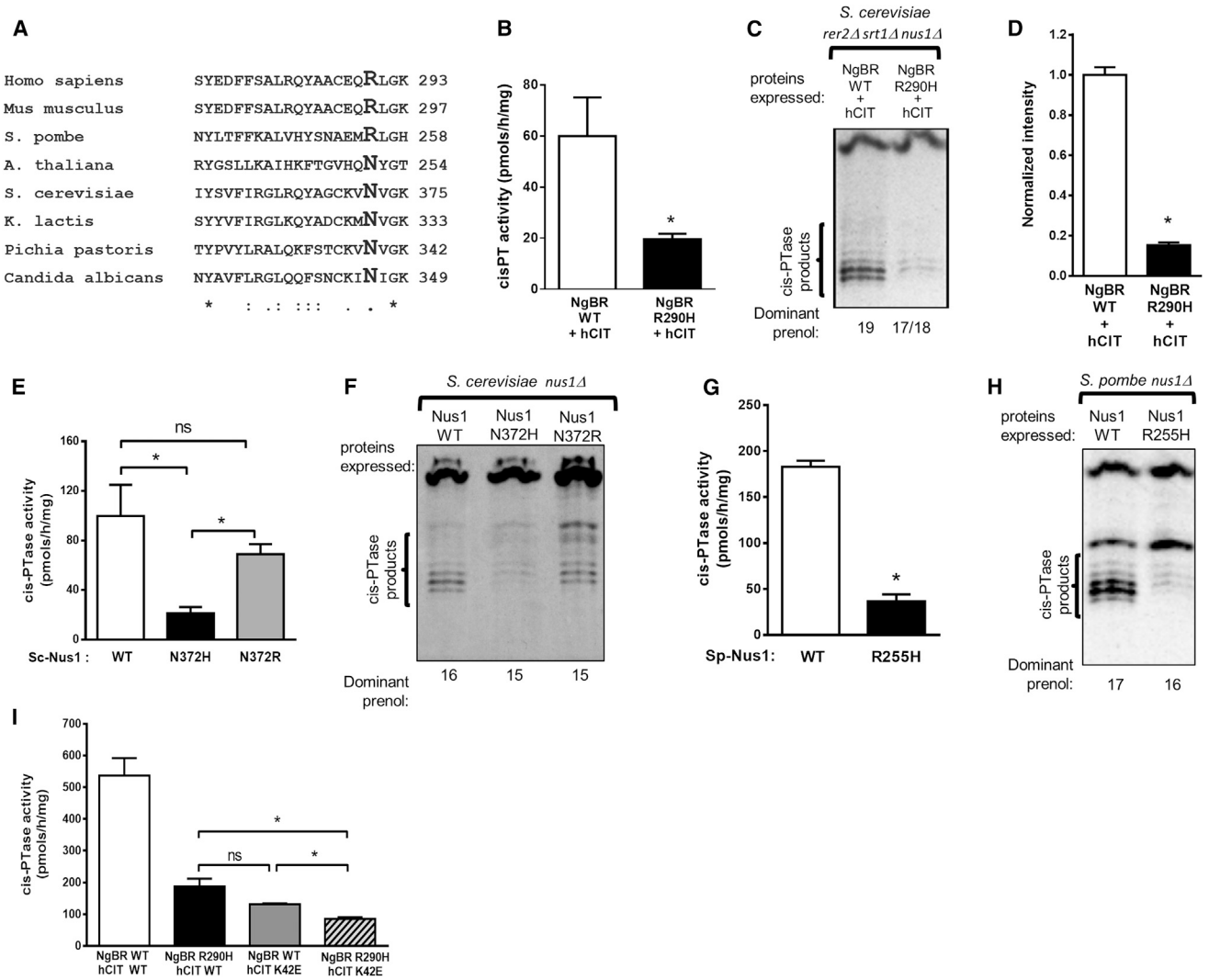

Figure 5. Characterization of NgBR/NUS1 Mutation in *S. cerevisiae* and *S. pombe*

(A) Amino acid alignment of the C terminus of NgBR orthologs. Arginine or asparagine is present at the fourth position from the C terminus.

(B and D) Shown are the *cis*-PTase activity measurements (B) and total dolichol level (D) measured from *rer2Δ, srt1Δ, nus1Δ S. cerevisiae* strain expressing hCIT and NgBR or NgBR-R290H by mass spectrometry.

(C) Reverse-phase TLC separation of *cis*-PTase products from *rer2Δ, srt1Δ, nus1Δ* triple deletion *S. cerevisiae* strain expressing the indicated constructs. About 15% of dolichol was detected in the NgBR mutant-expressing cells compared to wild-type NgBR.

(E and F) Shown are *cis*-PTase activity (E) and reverse-phase TLC separation (F) in *S. cerevisiae nus1Δ* strain expressing the indicated constructs.

(G and H) Shown are *cis*-PTase activity (G) and TLC separation of the products (H) in *S. pombe nus1Δ* strain expressing the indicated constructs. Mutated form of NgBR or Nus1-expressing cells show reduced *cis*-PTase activity. Not only reduced *cis*-PTase product, but also shortened chain length was detected in the mutated form of protein-expressed cells.

(I) *cis*-PTase activity in *rer2Δ, srt1Δ, nus1Δ S. cerevisiae* strain expressing NgBR and hCIT indicated constructs. Samples were not dephosphorylated prior to TLC analysis. Data are ± SE. *$p < 0.05$. See also Figure S3.

Genetic evidence for the importance of this interaction stems from data showing that NgBR knockout MEFs and patient fibroblasts harboring the R290H mutation exhibit increased free cholesterol levels. Since NPC2 is a soluble glycoprotein (Naureckiene et al., 2000) and glycosylation of NPC2 is important for its function (Chikh et al., 2004), it is feasible that in addition to a direct stabilizing effect of NgBR on NPC2, mutant NgBR can influence NPC2 glycosylation due to reduced *cis*-PTase activity contributing to this phenotype (Figure 6B). The interaction of NgBR with Nogo-B does not impact *cis*-PTase activity or cellular cholesterol content and may influence intracellular signaling pathways.

Little is known about the function of dolichol species in vivo besides its role as a glycan carrier, although in vitro evidence suggests that dolichol can modulate biophysical properties of membranes and serve as a cellular antioxidant (Surmacz and Swiezewska, 2011). Patients carrying a mutation in NgBR demonstrated altered ratios of dolichol in urine and in blood.

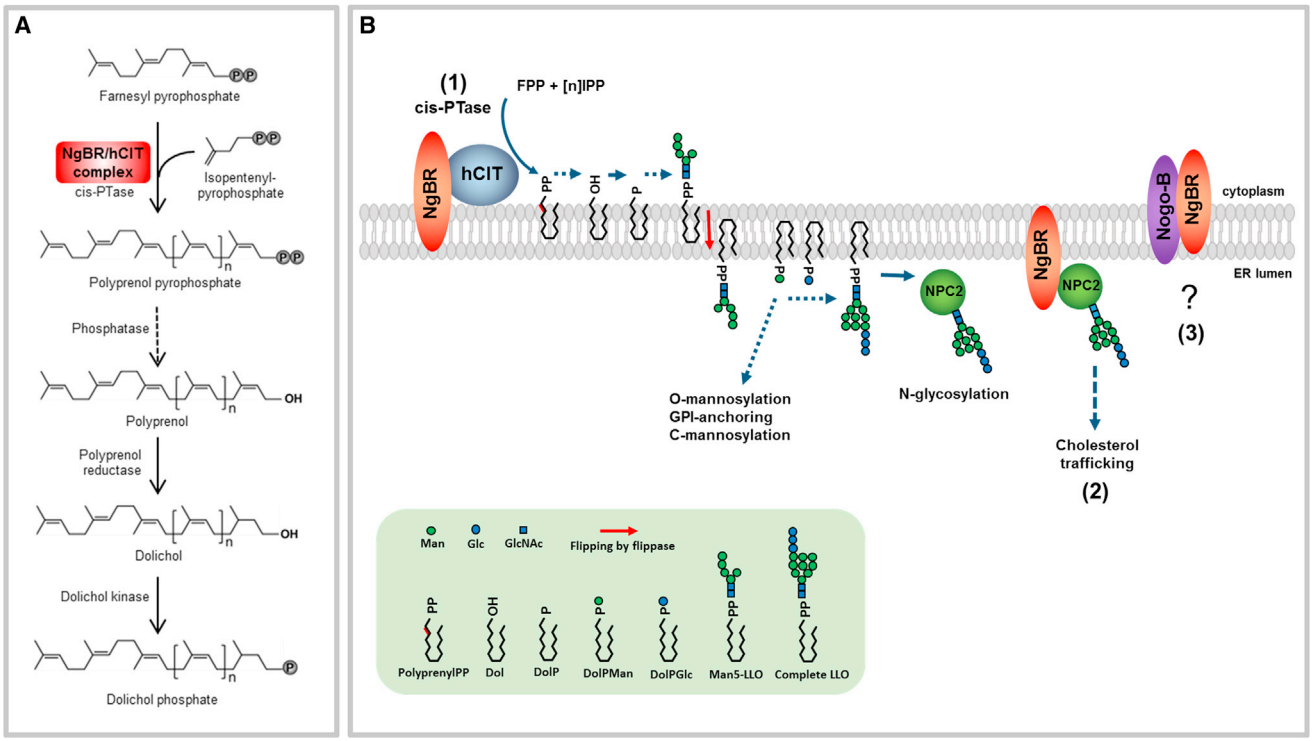

Figure 6. Functions of the NgBR/hCIT Complex in Cellular Metabolism

(A) The NgBR and hCIT complex promotes *cis*-PTase activity. NgBR/hCIT catalyzes the condensation of isopentenyl pyrophosphate with farnesyl pyrophosphate to generate a polyprenol pyrophosphate. Polyprenol diphosphate is dephosphorylated by unidentified phosphatase and reduced by polyprenol reductase (SRD5A3) to form dolichol. Finally, dolichol is phosphorylated by dolichol kinase prior to the synthesis of dolichol-linked sugars required for glycosylation pathways.

(B) (1) NgBR and hCIT assembly is essential for *cis*-PTase activity generating polyprenol pyrophosphate on the cytoplasmic leaflet of the ER membrane. Polyprenol pyrophosphate serves as an intermediate in synthesis of dolichol-linked saccharides. Dolichol-pyrophosphate tetradecasaccharide (LLO) is indispensable for protein N-glycosylation reactions. Dolichol-phosphate mannose (DolPMan) is also involved in O-mannosylation, GPI-anchor synthesis, and C-mannosylation. (2) NgBR influences cholesterol trafficking by directly interacting with NPC2 and indirectly via modifying NPC2 N-glycosylation. (3) The interaction between Nogo-B and NgBR does not influence glycosylation or cholesterol trafficking, and the function of this interaction remains to be clarified.

Although altered dolichol chain length ratios are important biomarkers in patients with mutations in hCIT/DHDDS and NgBR, alterations in dolichol chain length are unlikely to exert a dominant effect since lipid-linked oligosaccharides built on as few as 11 dolichol units seem to be efficient substrates in N-glycosylation reactions (Grabińska et al., 2010; Rush et al., 2010). However, the overall lower dolichol content of cell membranes not only directly affects glycosylation but can impair membrane structure and, in turn, affect multiple cellular processes including sterol biosynthesis. In summary, the development of a knockout strain of mice, the establishment of a NgBR/hCIT reconstitution system in yeast, and the discovery of a highly conserved mutation in the NgBR mutation in humans will assist in the further characterization of the cellular functions of this essential polyisoprene lipid.

EXPERIMENTAL PROCEDURES

Generation of NgBR Mouse Embryonic Fibroblasts

$NgBR^{f/f}$ was crossed with $NgBR^{+/\Delta}$; R26CreER (Badea et al., 2003), and primary MEFs were prepared from E13.5 embryos. Each MEF line was derived from an individual embryo. Isolated MEFs were immortalized using an SV40-large-T-expressing retrovirus obtained from Genecoepiea (LP-SV40T-LV105-0205) according to the manufacturer's protocol. Immortalized cells were maintained in Dulbecco's modified Eagle's medium (DMEM) with 1% penicillin/streptomycin containing 10% FBS. The genotypes of control MEFs and NgBR iKO MEFs used in this study are $NgBR^{f/+}$ and $NgBR^{+/\Delta}$; R26CreER. Both cell lines were treated with 1 μM 4-hydroxytamoxifen (Sigma) for more than 5 days to induce Cre recombination. mRNA or protein expression level was confirmed for each experiment. All experiments with $NgBR^{fl/fl}$ mice were approved by the Institutional Animal Care Use Committee at Yale School of Medicine.

Filipin Staining

Filipin staining was performed as previously described (Harrison et al., 2009). In brief, cells were fixed in 4% paraformaldehyde for 10 min and permeablized in 0.1% Triton X-100 for 5 min. Cells were then incubated with a 50 μg/ml concentration of filipin (Sigma, F4767) for 1 hr. As a positive control for induction of cholesterol accumulation, cells were treated for 8 hr with 1 μM U18666A (EMD Biosciences). Relative intensity of filipin staining was quantified by calculating average pixel intensity using Adobe Photoshop according to the following equation: average filipin intensity = total intensity above low threshold / number of pixels above low threshold (Pipalia et al., 2006).

Microsomal *cis*-PTase Activity Assay

For mammalian cells, crude microsomes were prepared as described before (Rush et al., 2010) with minor modification. *cis*-PTase activity in mammalian

cells was assayed as described before (Harrison et al., 2011) with minor modification. For *S. cerevisiae* and *S. pombe*, membrane fraction was prepared as described before (Szkopińska et al., 1997). *cis*-PTase assay using yeast membranes was performed as described (Szkopińska et al., 1997) with minor modifications. For a detailed description, please see the Supplemental Experimental Procedures.

[2-^{3}H]-Mannose Incorporation

D-[2-^{3}H]-mannose (15–30 Ci/mmol) was purchased from PerkinElmer. Cells were grown in 6-well dishes until 80%–90% confluent. Growth medium was replaced and incubated for 1 hr with glucose-free DMEM supplemented with 0.1 mg/ml glucose and 5% dialyzed fetal calf serum. Next, 5 μg/ml of tunicamycin was added to media as a control for inhibition of N-glycosylation. After 1 hr, 20 uCi/ml [2-^{3}H]-mannose was added and incubated for 4 hr at 37°C. Then, cells were washed with PBS and lysed in RIPA buffer. Cell lysates were then subjected to precipitation of proteins with 10% trichloroacetic acid (TCA) for 1 hr on ice. Precipitates were resuspended in 6 M Urea/SDS buffer and counted by scintillation.

Coimmunoprecipitation and Western Blot Analysis

Cos7 cells were transfected using Lipofectamine 2000 (Invitrogen) according to the manufacturer's protocol and harvested 48 hr after transfection. Cells were collected and lysed in IP buffer (IP buffer: 50 mM HEPES, 150 mM NaCl, 1 mM EDTA, 1% Triton X-100, 1.5 mg/ml protease inhibitor cocktail). Lysates were cleared at 12,000 rpm, and 20 μl of anti-HA agarose (Pierce) was used to pull down the HA-tagged protein from 1 mg of cell lysate. After incubation for 2 hr at 4°C, agarose beads were washed with IP buffer, resuspended in SDS loading buffer, and boiled for 5 min before western blotting.

Quantitative RT-PCR

Cells were collected in RLT buffer (QIAGEN). Total RNA were extracted using the RNeasy mini kit (QIAGEN), and 500 ng of total RNA was transcribed using superscript First-Strand Synthesis System with oligo dT primers (Invitrogen). Quantitative RT-PCR was performed using iQ SYBR Green Supermix (Bio-Rad) for the detection of fluorescence during amplification. Gapdh was used as an internal control. Expression of target genes was normalized to that of Gapdh using the comparative ΔCT method. Data are presented in relative expression to control ± SEM.

Human Subjects and DNA Analysis

The family of Roma origin was ascertained at the Department of Pediatrics of the First Faculty of Medicine, Charles University in Prague. Investigations were approved by the Institutional Review Board and conducted according to the Declaration of Helsinki principles. Written, informed consent was obtained from all subjects. Participants provided urine and venous blood. Skin biopsy was obtained from both affected individuals, and skin fibroblasts were cultured according to standard protocols. Autopsy material has been collected from deceased proband II.3. Genomic DNA was isolated from blood using standard technology and analyzed as described in the Supplemental Experimental Procedures.

Yeast Strains, Plasmids, and Culture Methods

S. cerevisiae strains used in these studies include: KG404-16B (*nus1Δ*/pNEV-Glc*is*PT), KG405 (*rer2Δ*, *srt1Δ*, *nus1Δ*/pNEV-Glc*is*PT), and BY4742 and their derivatives. The *S. pombe* strain used was KGSP16 (Sp*nus*1Δ REP42GW-Glc*is*PT). For yeast culture methods and detailed information about the strains, please see the Supplemental Experimental Procedures.

Analysis of Dolichols by LC-MS

Serum and urine from family members and healthy unrelated controls were collected according to standard protocols. The samples were frozen at −80°C until the lipid extraction and the analysis. The lipid fraction was isolated from membranes isolated of S. *cervisiae* (2 mg of proteins) or fibroblast (0.5 mg of proteins) as described before (Grabińska et al., 2005), and dolichol content was analyzed by liquid chromatography and mass spectrometry (LC-MS) (Guan and Eichler, 2011; Wen et al., 2013). For a detailed description, please see the Supplemental Experimental Procedures.

SUPPLEMENTAL INFORMATION

Supplemental Information includes Supplemental Experimental Procedures, three figures, and one table and can be found with this article online at http://dx.doi.org/10.1016/j.cmet.2014.06.016.

AUTHOR CONTRIBUTIONS

E.J.P. and K.A.G. contributed equally to all aspects of this paper: E.J.P. characterized NgBR deficient mice and performed all mammalian cell based studies and cloning/plasmid construction, and K.A.G. developed yeast strains and *cis*-PTase characterization in vivo and in vitro. Both authors contributed to the writing and editing of the manuscript. Z.G. and R.W. contributed to MS analysis of urinary and serum dolichol levels and the writing of the manuscript. V.S., H. Hartmannová, and K.H. performed genotyping, linkage analysis, homozygosity mapping, and exome sequencing. V.B., J.S., N.O., H. Hansíková, and H. Hůlková contributed to acquisition of clinical specimens and phenotypic characterization of patients. T.H. and J.Z. were responsible for clinical and diagnostic assessment of affected patients. L.J. performed high-resolution imaging of Nogo-B in patient cells. W.C.S., E.J.P., K.A.G., and S.K. were responsible for concept development and preparation of the manuscript. S.K. was responsible for overseeing the genetic aspects of the study, and W.C.S. was responsible for overall integration and execution of the scientific approaches.

ACKNOWLEDGMENTS

We would like to thank Dr. Patrick Lusk (Department of Cell Biology, Yale School of Medicine) for giving us access to a dissection microscope for yeast tetrad separation and Marcela Michaličková (General Faculty Hospital Prague) for ophthalmologic investigations. This work was supported by grants R01 HL64793, R01 HL61371, R01 HL081190, RO1 HL096670, and P01 HL70295 from the National Institutes of Health to W.C.S. Z.G. and the mass spectrometry facility in the Department of Biochemistry, Duke University Medical Center were supported by a LIPID MAPS glue grant (GM-069338) from the National Institutes of Health. V.S., H. Hartmannová, K.H., V.B., J.S., N.O., H. Hansíková, T.H., J.Z., H. Hůlková, and S.K. were supported by the Charles University institutional programs PRVOUK-P24/LF1/3, UNCE 204011, and SVV2014/260 022 and by BIOCEV – Biotechnology and Biomedicine Centre of the Academy of Sciences and Charles University (CZ.1.05/1.1.00/02.0109) from the European Regional Development Fund. Specific support was provided by grants NT13116-4/2012 and NT12166-5/2011 from the Ministry of Health of the Czech Republic.

Received: March 11, 2014
Revised: May 28, 2014
Accepted: June 14, 2014
Published: July 24, 2014

REFERENCES

Badea, T.C., Wang, Y., and Nathans, J. (2003). A noninvasive genetic/pharmacologic strategy for visualizing cell morphology and clonal relationships in the mouse. J. Neurosci. *23*, 2314–2322.

Cantagrel, V., Lefeber, D.J., Ng, B.G., Guan, Z., Silhavy, J.L., Bielas, S.L., Lehle, L., Hombauer, H., Adamowicz, M., Swiezewska, E., et al. (2010). SRD5A3 is required for converting polyprenol to dolichol and is mutated in a congenital glycosylation disorder. Cell *142*, 203–217.

Cenedella, R.J. (2009). Cholesterol synthesis inhibitor U18666A and the role of sterol metabolism and trafficking in numerous pathophysiological processes. Lipids *44*, 477–487.

Chikh, K., Vey, S., Simonot, C., Vanier, M.T., and Millat, G. (2004). Niemann-Pick type C disease: importance of N-glycosylation sites for function and cellular location of the NPC2 protein. Mol. Genet. Metab. *83*, 220–230.

Fujihashi, M., Zhang, Y.W., Higuchi, Y., Li, X.Y., Koyama, T., and Miki, K. (2001). Crystal structure of cis-prenyl chain elongating enzyme, undecaprenyl diphosphate synthase. Proc. Natl. Acad. Sci. USA *98*, 4337–4342.

Grabińska, K., Sosińska, G., Orłowski, J., Swiezewska, E., Berges, T., Karst, F., and Palamarczyk, G. (2005). Functional relationships between the Saccharomyces cerevisiae cis-prenyltransferases required for dolichol biosynthesis. Acta Biochim. Pol. *52*, 221–232.

Grabińska, K.A., Cui, J., Chatterjee, A., Guan, Z., Raetz, C.R., Robbins, P.W., and Samuelson, J. (2010). Molecular characterization of the cis-prenyltransferase of Giardia lamblia. Glycobiology *20*, 824–832.

Guan, Z., and Eichler, J. (2011). Liquid chromatography/tandem mass spectrometry of dolichols and polyprenols, lipid sugar carriers across evolution. Biochim. Biophys. Acta *1811*, 800–806.

Guo, R.T., Ko, T.P., Chen, A.P., Kuo, C.J., Wang, A.H., and Liang, P.H. (2005). Crystal structures of undecaprenyl pyrophosphate synthase in complex with magnesium, isopentenyl pyrophosphate, and farnesyl thiopyrophosphate: roles of the metal ion and conserved residues in catalysis. J. Biol. Chem. *280*, 20762–20774.

Harrison, K.D., Miao, R.Q., Fernandez-Hernándo, C., Suárez, Y., Dávalos, A., and Sessa, W.C. (2009). Nogo-B receptor stabilizes Niemann-Pick type C2 protein and regulates intracellular cholesterol trafficking. Cell Metab. *10*, 208–218.

Harrison, K.D., Park, E.J., Gao, N., Kuo, A., Rush, J.S., Waechter, C.J., Lehrman, M.A., and Sessa, W.C. (2011). Nogo-B receptor is necessary for cellular dolichol biosynthesis and protein N-glycosylation. EMBO J. *30*, 2490–2500.

He, P., Ng, B.G., Losfeld, M.E., Zhu, W., and Freeze, H.H. (2012). Identification of intercellular cell adhesion molecule 1 (ICAM-1) as a hypoglycosylation marker in congenital disorders of glycosylation cells. J. Biol. Chem. *287*, 18210–18217.

Kasapkara, C.S., Tümer, L., Ezgü, F.S., Hasanoğlu, A., Race, V., Matthijs, G., and Jaeken, J. (2012). SRD5A3-CDG: a patient with a novel mutation. Eur. J. Paediatr. Neurol. *16*, 554–556.

Miao, R.Q., Gao, Y., Harrison, K.D., Prendergast, J., Acevedo, L.M., Yu, J., Hu, F., Strittmatter, S.M., and Sessa, W.C. (2006). Identification of a receptor necessary for Nogo-B stimulated chemotaxis and morphogenesis of endothelial cells. Proc. Natl. Acad. Sci. USA *103*, 10997–11002.

Naureckiene, S., Sleat, D.E., Lackland, H., Fensom, A., Vanier, M.T., Wattiaux, R., Jadot, M., and Lobel, P. (2000). Identification of HE1 as the second gene of Niemann-Pick C disease. Science *290*, 2298–2301.

O'Gorman, S., Dagenais, N.A., Qian, M., and Marchuk, Y. (1997). Protamine-Cre recombinase transgenes efficiently recombine target sequences in the male germ line of mice, but not in embryonic stem cells. Proc. Natl. Acad. Sci. USA *94*, 14602–14607.

Pipalia, N.H., Huang, A., Ralph, H., Rujoi, M., and Maxfield, F.R. (2006). Automated microscopy screening for compounds that partially revert cholesterol accumulation in Niemann-Pick C cells. J. Lipid Res. *47*, 284–301.

Rush, J.S., Matveev, S., Guan, Z., Raetz, C.R., and Waechter, C.J. (2010). Expression of functional bacterial undecaprenyl pyrophosphate synthase in the yeast rer2Delta mutant and CHO cells. Glycobiology *20*, 1585–1593.

Sato, M., Sato, K., Nishikawa, S., Hirata, A., Kato, J., and Nakano, A. (1999). The yeast RER2 gene, identified by endoplasmic reticulum protein localization mutations, encodes cis-prenyltransferase, a key enzyme in dolichol synthesis. Mol. Cell. Biol. *19*, 471–483.

Schenk, B., Rush, J.S., Waechter, C.J., and Aebi, M. (2001). An alternative cis-isoprenyltransferase activity in yeast that produces polyisoprenols with chain lengths similar to mammalian dolichols. Glycobiology *11*, 89–98.

Surmacz, L., and Swiezewska, E. (2011). Polyisoprenoids - Secondary metabolites or physiologically important superlipids? Biochem. Biophys. Res. Commun. *407*, 627–632.

Szkopińska, A., Grabińska, K., Delourme, D., Karst, F., Rytka, J., and Palamarczyk, G. (1997). Polyprenol formation in the yeast Saccharomyces cerevisiae: effect of farnesyl diphosphate synthase overexpression. J. Lipid Res. *38*, 962–968.

Wen, R., Lam, B.L., and Guan, Z. (2013). Aberrant dolichol chain lengths as biomarkers for retinitis pigmentosa caused by impaired dolichol biosynthesis. J. Lipid Res. *54*, 3516–3522.

Xiang, Y., Zhang, X., Nix, D.B., Katoh, T., Aoki, K., Tiemeyer, M., and Wang, Y. (2013). Regulation of protein glycosylation and sorting by the Golgi matrix proteins GRASP55/65. Nat Commun *4*, 1659.

Yu, L., Peña Castillo, L., Mnaimneh, S., Hughes, T.R., and Brown, G.W. (2006). A survey of essential gene function in the yeast cell division cycle. Mol. Biol. Cell *17*, 4736–4747.

Zelinger, L., Banin, E., Obolensky, A., Mizrahi-Meissonnier, L., Beryozkin, A., Bandah-Rozenfeld, D., Frenkel, S., Ben-Yosef, T., Merin, S., Schwartz, S.B., et al. (2011). A missense mutation in DHDDS, encoding dehydrodolichyl diphosphate synthase, is associated with autosomal-recessive retinitis pigmentosa in Ashkenazi Jews. Am. J. Hum. Genet. *88*, 207–215.

Züchner, S., Dallman, J., Wen, R., Beecham, G., Naj, A., Farooq, A., Kohli, M.A., Whitehead, P.L., Hulme, W., Konidari, I., et al. (2011). Whole-exome sequencing links a variant in DHDDS to retinitis pigmentosa. Am. J. Hum. Genet. *88*, 201–206.